Research article

Development and characterization of monoclonal antibodies recognizing nucleocapsid protein of multiple SARS-CoV-2 variants

Hongyu Qiu [*], Xin-Yong Yuan, Kimberly Holloway, Heidi Wood, Teresa Cabral, Chris Grant, Peter McQueen, Garrett Westmacott, Daniel R. Beniac, Lisa Lin, Michael Carpenter, Darwyn Kobasa, Tom Gräfenhan [**],[1], Ian Wayne Cheney [***]

National Microbiology Laboratory, Public Health Agency of Canada, 1015 Arlington Street, Winnipeg, MB, R3E 3R2, Canada

ARTICLE INFO

ABSTRACT

Rapid antigen test (RAT) is widely used for SARS-CoV-2 infection diagnostics. However, test sensitivity has decreased recently due to the emergence of the Omicron variant and its sublineages. Here we developed a panel of SARS-CoV-2 nucleocapsid protein (NP) specific mouse monoclonal antibodies (mAbs) and assessed their sensitivity and specificity to important SARS-CoV-2 variants. We identified seven mAbs that exhibited strong reactivity to SARS-CoV-2 variants and recombinant NP (rNP) by Western immunoblot or ELISA. Their specificity to SARS-CoV-2 was confirmed by negative or low reactivity to rNPs from SARS-CoV-1, MERS, and common human coronaviruses (HCoV-HKU1, HCoV–CO43, HCoV-NL63, and HCoV-229E). These seven mAbs were further tested by immunoplaque assay against selected variants of concern (VOCs), including two Omicron sublineages, and five mAbs (F461G13, F461G7, F459G7, F457G3, and F461G6), showed strong reactions, warranting further suitability testing for the development of diagnostic assay.

1. Introduction

The emergence of SARS-CoV-2 variant B1.1.529 (Omicron) has dramatically altered the course of the Coronavirus Disease 2019 (COVID-19) pandemic. Omicron replaced the previous variant of concern (VOC) B.1.617.2 (Delta) and rapidly spread worldwide since first being detected in November 2021. Its sublineages are currently the dominant variants by far [1,2].

In contrast to the original strain and the other VOCs, Omicron and its sublineages are less virulent. Multiple clinical studies have shown that Omicron-infected individuals have reduced risks of hospitalization and experience less severe consequences such as oxygen supplementation, ventilation, or death [3–8].

With the progress of vaccination and the prevalence of Omicron, the COVID-19-related mortality rate has decreased significantly

---

[9–13]. Public health measures, such as travel restrictions, wearing masks in enclosed spaces, and keeping social distance, have been gradually lifted by most governments. However, due to its high transmissibility [14,15], Omicron-related severe disease and death are still high. There were over 1.2 million confirmed deaths worldwide, including over 250,000 in the US in 2022, when Omicron and its sublineages dominated the pandemic [16,17]. In comparison, the annual total deaths linked to seasonal influenza was 650,000 globally, as estimated by the World Health Organization [18,19]. The high-risk populations for severe COVID-19 diseases remain the elderly, people with obesity or with comorbidities such as diabetes, cardiovascular diseases or high blood pressure [11,20,21]. Therefore, other than vaccination, preventive actions such as COVID-19 testing and seeking prompt treatment after a positive diagnosis are recommended by the CDC to protect high-risk individuals [22].

As the gold standard for COVID-19 diagnostics, Reverse Transcription Quantitative PCR (RT-qPCR) is highly sensitive and accurate. However, it requires specific instruments and trained technologists, and the limited number of available diagnostic labs and slow turnaround time do not fit the test demands during COVID-19 waves. In contrast, the RAT (Rapid Antigen Test) based on antigen-specific antibodies is relatively inexpensive, easy to operate, quick to obtain results, and highly specific [23–25]. Although not as sensitive as RT-qPCR, RAT can be repeated for several days to improve the detection rates [26–28]. This test has been demonstrated to reduce transmission and prevent hospital admissions [29]. Furthermore, the rapid diagnosis of vulnerable people with COVID-19 symptoms provides an early alert for treatment with antiviral drugs such as Paxlovid or Molnupiravir. Studies have shown that treatment during the first several days of infection significantly reduces the risk of disease progression, hospitalization, and death [30–33]. The challenge for the use of current RAT kits is the drastically reduced sensitivity to Omicron lineages compared to previous variants [28,34–36]. It is believed that mutations in NP are largely responsible for the reduced sensitivity, since almost all the RAT kits are based on mAbs-NP interaction [37]. Therefore, it is necessary to constantly monitor the performance of current RAT kits and develop new kits based on antibodies recognizing emerging variants.

In this study, we report the generation of a panel of NP-specific monoclonal antibodies using SARS-CoV-2 immunized mice. After screening against rNP and inactivated virus variants, seven mAbs with high affinity to SARS-Cov-2 variants were identified. Further studies confirmed their specificity to SARS-CoV-2 virus by screening against SARS-CoV-1, MERS, and common human coronaviruses. Five of the mAbs demonstrated strong reactivity to all tested VOCs, including B.1.1.7, B.1.351, P.1, B.1.617.2, B.1.1.529 (Omicron) and Omicron subvariant BA2. Further testing of the five mAbs confirmed their response to the recently circulated Omicron sublineage JN.1, supporting their potential use in antigen test development.

2. Materials and methods

2.1. Generation of SARS-CoV-2 specific mAb hybridoma clones and screening

Mice were housed in an animal facility accredited by the Association for Assessment and Accreditation of Laboratory Animal Care (AAALAC) and approved by the Institutional Animal Care and Use Committee (IACUC) of the National Microbiology Laboratory Canada.

SARS-CoV-2 virus reference strain (hCoV-19/Canada/ON_ON-VIDO-01-2/2020, EPI_ISL_425177) antigen preparation, mouse immunization and hybridoma generation have been described in a previous publication [38]. Culture supernatants of selected hybridoma clones were tested against γ-irradiated SARS-CoV-2, recombinant Spike protein (rSP), and rNP (generated in-house by a mammalian cell expression system), by ELISA and Western Immunoblot, followed by surrogate virus neutralization testing and plaque reduction Neutralization Tests (PRNT).

rNP-positive clones were designated nucleocapsid protein-specific mAbs, and were subcloned, cultured, and expanded in Cytiva CCM1 serum-free hybridoma media (Fisher Scientific, Toronto, ON, Canada). The culture supernatants were harvested, and mAbs were purified with HiTrap™ Protein G column (Sigma-Aldrich, Oakville, ON, Canada) per the manufacturer's instructions.

2.2. Antibody de novo amino acid sequence determination and analysis

Antibody amino acid sequences were determined as described previously [38]. Briefly, purified individual mAbs were reduced, alkylated, and deglycosylated using DTT, iodoacetamide, and PNGaseF sequentially. Then, seven aliquots (10 μg each) were separately digested with pepsin (used at < pH2 and > pH2), chymotrypsin, Glu-C, Lys-C, Asp-N (all from Promega) and trypsin (Pierce, ThermoFisher Scientific, Waltham, MA). The digested antibody samples were then concentrated and analyzed by nanoflow-liquid chromatography-tandem mass spectrometry (nLC-MS/MS) using a Orbitrap Q-Exactive Plus connected in-line with an Easy nLC 1000 (Thermo Fisher Scientific) using an EASY-Spray ES903 C18 column (50 cm × 75 μm x 2 μm, Thermo Fisher Scientific). Data dependant acquisition method was used over a 120 min nLC gradient per sample. Raw mass spectrometry files were analyzed using PEAKS AB software (Bioinformatics Solutions Inc., Waterloo, ON, Canada). Complementarity-determining regions (CDR) were assigned by the PEAKS AB software automatically based on a self-contained database provided with PEAKS AB. IgBLAST (https://www.ncbi.nlm.nih.gov/igblast/index.cgi) was used for germline gene alignment and allele determination based on protein sequences.

2.3. Purified antibody titer analysis by ELISA

Purified mAbs were tested for antigen binding titers to rNPs of SARS-CoV-2 variants (Sino Biological US., Wayne, PA; or ACROBiosystems, Newwark, DE) by end-point-ELISA (EPE). Briefly, 96-well ELISA plates were coated with rNPs (100 ng/well), then blocked with blocking buffer (0.2 % skim milk+0.2 % FBS in PBS) and incubated with two-fold serial dilutions of purified mAbs with a starting

concentration of 10 μg/well. HRP-conjugated goat anti-mouse IgG (Southern Biotechnology, Birmingham, AL) was added to each well in a 1:2000 dilution. After incubation, the colour reaction was developed using 1 mM ABTS (Sigma-Aldrich) and quantified at 405 nm using a microplate reader. Endpoint titers of each sample to SARS-CoV-2 rNP were determined as the lowest concentrations of the wells at which the optical density (OD) was threefold higher than the negative control. Immunized and pre-immunized mouse sera at 1:2000 dilutions were used as positive and negative controls, respectively.

ELISA to rNPs of SARS-CoV-1, MERS, and common coronaviruses were conducted similarly to the EPE, except that the starting concentrations of tested mAbs were at 1:100 dilution (4–10 μg/mL).

2.4. Western immunoblot analysis

Antibody specificity to SARS-Cov-2 NP was validated by Western immunoblot. rNP (in-house produced or from Sigma-Aldrich) were resolved by SDS-polyacrylamide gel electrophoresis (PAGE) using 4–20 % Mini-PROTEAN TGX gels (Bio-Rad Laboratories Canada, Mississauga, ON, Canada) and transferred onto polyvinylidene fluoride (PVDF) membranes (ThermoFisher Scientific) by electroblotting. The membranes were blocked with 5 % skim milk in Tris-buffered saline (TBS) for 1 h at room temperature then incubated with purified mAb at 0.8 μg/mL for 1 h at room temperature. The membrane was washed three times with TBS containing 0.05 % Tween-20 (TBST). The secondary antibody 1:5000 HRP-conjugated goat anti-mouse IgG (SouthernBiotech) in TBST was incubated with the membrane for 1 h, washed as described previously, then developed using DAB substrate (ThermoFisher Scientific).

2.5. Immunoplaque assay

Vero E6 or Vero E6/TMPRSS2 cells (BPS Bioscience, San Diego, CA) were seeded into 12-well tissue culture plates at a density of 3.3×10^5 cells/well then incubated overnight at 37 °C with 5 % CO2. Vero E6 cells were used for all SARS-CoV-2 variants tested except for Omicron BA.2, which required Vero E6/TMPRSS2 cells for foci production. The following day medium was removed, and an inoculum of 1000 plaque-forming units (pfu) was added to each well. After 1 h of incubation, the monolayers were overlaid with 1.5 mL of 1.5 % carboxymethylcellulose (CMC) in modified Eagle's medium (4 % FBS, 1 % ʟ-glutamine, 1 % non-essential amino acids, 0.75 % sodium bicarbonate). Plates infected with the reference strain or the variants except for Omicron BA.1 or BA.2 were incubated overnight at 37 °C, 5 % CO2. Plates infected with BA.1 or BA.2 were incubated for 48 h. After 24 or 48 h, the CMC overlay was removed, and cells were fixed with 10 % buffered formalin phosphate.

Monolayers were rinsed in PBS and treated with a permeabilization buffer (PBS pH 7.2; 0.15 % glycine, 0.5 % Triton X-100) for 20 min at room temperature. Plates were then manually washed three times with wash buffer (PBS containing 0.5 % Tween-20) and incubated with monoclonal antibodies (1 μg/5 mL) in dilution buffer (PBS, 10 % horse serum, 0.4 % Tween-80) for 1 h at room temperature. After washing, the fixed monolayers were treated with 1:2000 diluted HRP conjugated goat anti-mouse IgG, Fcγ fragment antibody (Jackson ImmunoResearch, West Grove, PA) for 1 h at room temperature. Fixed monolayers were washed, and KPL TrueBlue™ Peroxidase Substrate (SeraCare, Milford, MA) was added to each well. After a 30 min incubation at room temperature, monolayers were washed and air dried.

3. Results

3.1. Development and screening of SARS-CoV-2 nucleocapsid protein-specific monoclonal antibodies

Four mice were immunized and boosted with formalin-inactivated SARS-CoV-2 for hybridoma development. Forty-four clones were immunoreactive in ELISA against either γ-irradiated SARS-CoV-2, rSP, or rNP. Their isotypes were determined using a murine isotyping dipstick test (Roche Diagnostics, Indianapolis, IND). Following further confirmation by western immunoblot, thirteen clones that only reacted to rNP were picked for two rounds of subcloning. Two clones, F458G1 and F461G12, stopped producing antibodies

Table 1
Sequence analysis of anti-nucleocapsid protein antibodies.[a].

NP[b] specific mAbs	V gene (Heavy Chain)	Number of mismatches gaps and identity compared to germline (Heavy Chain)	V gene (Light Chain)	Number of mismatches gaps and identity compared to germline (Light Chain)
F457G2	IGHV9-3-1*01	26 (75.7 %)	IGKV12-46*01	7 (92.6 %)
F457G3	IGHV3-2*02	31 (72.1 %)	IGKV1-88*01	1 (99 %)
F457G6	IGHV9-3-1*01	43 (60.2 %)	IGKV5-39*01	16 (83.2 %)
F457G9	IGHV3-2*02	20 (81.7 %)	IGKV1-88*01	1 (99 %)
F457G10	IGHV3-2*02	5 (94.9 %)	IGKV1-88*01	1 (99 %)
F457G12	IGHV3-2*02	9 (90.9 %)	IGKV1-88*01	1 (99 %)
F459G7	IGHV9-3-1*01	21 (80.6 %)	IGKV6-20*01	11 (88.4 %)
F461G5	IGHV5-6-4*01	2 (97.9 %)	IGLV1*01	4 (95.7 %)
F461G6	IGHV14-3*02	9 (90.8 %)	IGKV2-137*01	9 (91 %)
F461G7	IGHV14-3*02	7 (92.9 %)	IGKV2-137*01	3 (97 %)
F461G13	IGHV13-2*02	23 (77.2 %)	IGKV12-44*01	10 (89.5 %)

[a] the germline genes were based on the highest scores in the alignments.
[b] NP: nucleocapsid protein.

during subculturing and were discontinued. The remaining eleven subcloned hybridomas were cultured for large-scale production to analyze antigen specificity, antigen affinity, virus plaque detection, and antibody sequences.

3.2. Antibody sequence analysis

Anti-SARS-CoV-2 antibody amino acid sequences were determined using mass spectrometry-based *de-novo* sequencing of purified monoclonal antibody digests. Template sequences for each antibody were exported from PEAKS AB and considered the primary amino acid sequence. All eleven antibody sequences were generated from the results of two replicate digestion sets. Each sequence was evaluated manually for annotation of CDR and amino acid confidence. All the amino acids in heavy and light chain sequences were identified with >95 % confidence.

The sequences of the eleven anti-NP mAbs used five heavy chain-variable genes, with the VH3-2*02 most frequently used by four mAbs (F457G3, F457G9, F457G10 and F457G12), followed by VH9-3-1*01, used by three mAbs (F457G2, F457G6, and F459G7) (Table 1). While the light-chain of the eleven mAbs used seven light-chain-variable genes, with the VK1-88*01 used by four mAbs (F457G3, F457G9, F457G10 and F457G12), followed by VK2-137*01, used by two mAbs, and F461G5 used Vλ1*01 gene. The sequence identity to germline varied from 60.2 % to 97.9 % for heavy chains and 83.2 %–99 % for light chains, respectively. The broad range of sequence identity to the germline genes is consistent with repeating exposure to the antigen. The same heavy and light chain genes were used by F457G3, F457G9, F457G10 and F457G12 (VH3-2*02 and VK1-88*01), and F461G6 and F461G7 (VH14-3*02 and VK2-137*01) respectively, suggesting they were derived from related hybridoma clones.

3.3. Antibody reactivity to multiple SARS-CoV-2 variants

Eleven mAbs were tested against original SARS-CoV-2 (Wuhan strain) rNP and selected γ-irradiated SARS-CoV-2 variants. The bands were assessed based on molecular weights, and the intensity was graded on a 5-point scale (- to ++++) (Table 2). As indicated, all eleven mAbs reacted to SARS-CoV-2 (Wuhan) rNP, and most showed medium to strong reactivity to 1×10^4 pfu viruses. However, four mAbs, F457G9, F457G10, F457G12, and F461G5, did not react to the SARS-CoV-2 reference strain, B.1.525, and four VOCs (B.1.1.7, B.1.351, P.1, and B.1.617.2). In contrast, the remaining seven mAbs showed weak (+) to strong (+++) reactivity to the reference strain, B.1.1.7, B.1.351, and B.1.525. Five mAbs reacted strongly to P.1 (+++, or ++++). However, only two mAbs (F461G6 and F461G7) showed reactivity to B.1.617.2.

3.4. Antibody reactivity to nucleocapsid proteins from common human coronaviruses, SARS-CoV-1, and MERS

Potential cross-reactivity of eleven mAbs to rNPs from four common human coronaviruses (HCoV-HKU1, HCoV-OC43, HCoV-NL63, and HCoV-229E), SARS-CoV-1, and MERS were tested by ELISA. Naïve rabbit polyclonal antibody and mouse mAb against an irrelevant antigen were used as the negative controls, while rabbit pAbs against selected rNPs were used as the positive controls. For rNPs of MERS, HCoV-HKU1, HCoV-OC43, HCoV-NL63, and HCoV-229E, the OD values of tested samples at 1:100 dilution (mAb concentration at 4–10 μg/mL) ranged from 0.06 to 0.07, similar to the negative mAb control (Fig. 1A). In comparison, the positive controls at 1:100 dilution showed strong reactions to all rNPs, with OD values at ~3 to HCoV-HKU1 and HCoV-OC43, over 1.5 to HCoV-NL63 and HCoV-229E, and 0.6 to MERS, respectively. Moreover, HCoV-HKU1 and HCoV-OC43 pAbs at 1:51200 dilution, NL63 pAb at 1:12800 and 229E pAbs and 1:3200 dilution, and MERS pAb at the max dilution (1:204800) still showed higher OD values than those of the SARS-CoV-2 NP mAb samples at 1:100 dilution (Fig. 1A). In addition, the tested samples showed a strong reaction to SARS-CoV-2 rNP (Wuhan strain) in the End-Point-ELISA (Fig. 1B)

Interestingly, most of the tested mAbs showed dose-dependent reactivity to SARS-Cov-1 rNP, with the ODs ranging from 0.06

Table 2
Western immunoblot of mAbs to recombinant NP and SARS-CoV-2 variants

mAbs	SARS-CoV-2 rNP[b] (0.1 μg/lane)	SARS-CoV-2 reference strain[c,d] (1 × 10⁴ pfu/lane)	B.1.1.7 (Alpha)[d] (1 × 10⁴ pfu/lane)	B.1.351 (Beta)[d] (1 × 10⁴ pfu/lane)	P.1 (Gamma)[d] (1 × 10⁴ pfu/lane)	B.1.617.2 (Delta)[d] (1 × 10⁴ pfu/lane)	B.1.525 (Eta)[d] (1 × 10⁴ pfu/lane)
F457G2	+	++	+	++	+++	-	++
F457G3	+++	++	+	++	++	–	++
F457G6	+++	++	++	++	+++	-	++
F457G9	+++	-	-	-	-	-	-
F457G10	+++	-	-	-	-	-	-
F457G12	+++	-	-	-	-	-	-
F459G7	+++	+	+	++	+	-	++
F461G5	+++	-	-	-	-	-	-
F461G6	++	++	++	+++	++++	++	++
F461G7	++	+	+	++	++++	+	++
F461G13	++	++	++	+++	++++	-	+++

a, marks -, +, ++, +++, and ++++ were based on the band density visualized by experienced technician. -: no band observed. b, recombinant nucleocapsid protein of the original strain (Wuhan strain); c, gamma-irradiated reference strain (hCoV-19/Canada/ON_ON-VIDO-01-2/2020, EPI_ISL_425177); d, all strains were loaded at 1×10^4 pfu/lane for SDS-PAGE.
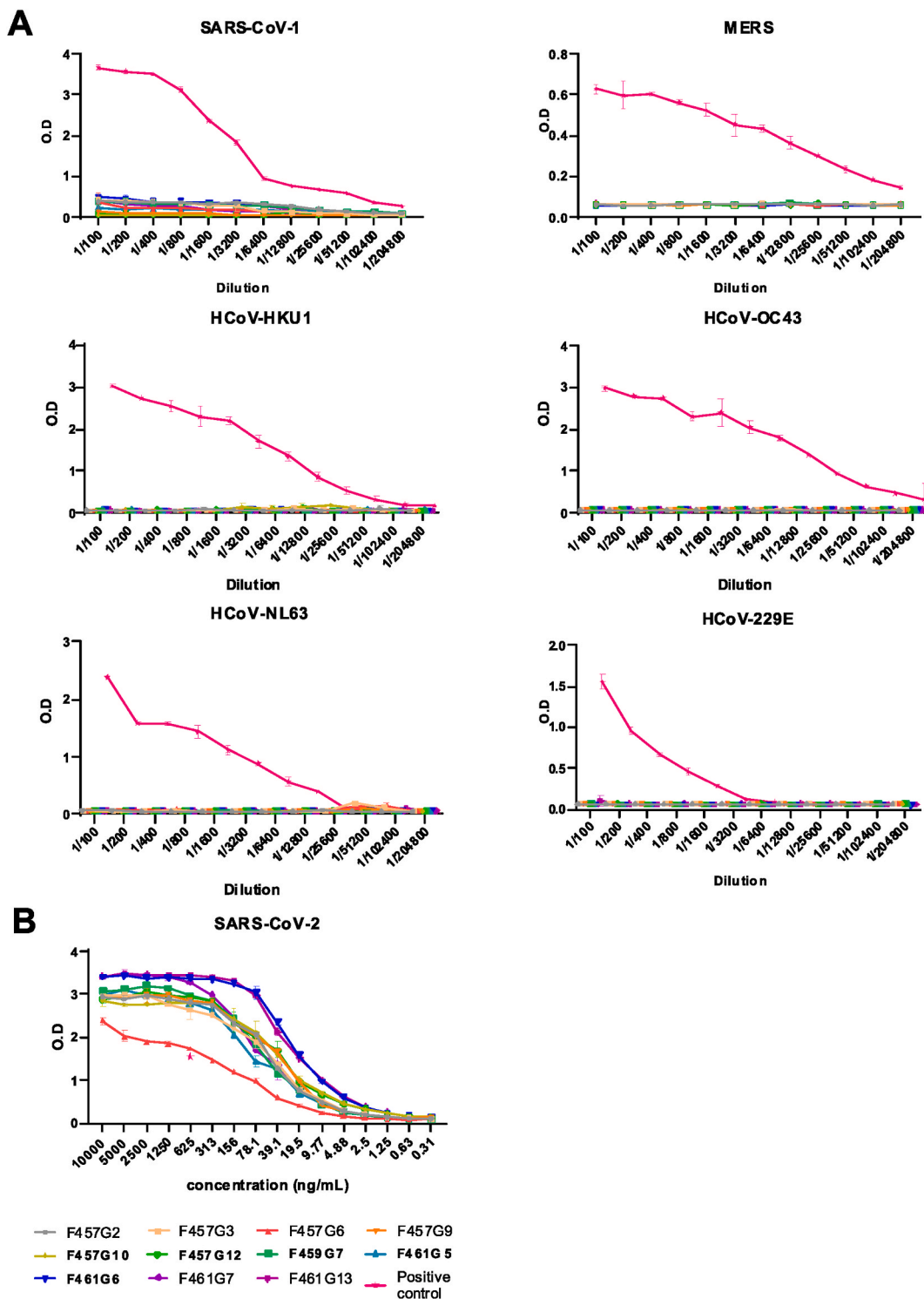
Fig. 1. Cross-reactivity of SARS-CoV-2 nucleocapsid protein mAbs to rNPs from SARS-Cov-1, MERS, and Common human coronaviruses (HCoV). Fig. 1A, ELISA was conducted to test cross-reactivity of eleven mAbs to recombinant nucleocapsid proteins (rNPs) from SARS-1, MERS, and HCoV-HKU1, -OC43, -NL63, and -229E, respectively. OD values of serial diluted mAbs were compared to positive control (rabbit polyclonal antibodies against each of the rNPs). Naïve rabbit polyclonal antibody and irrelevant mouse mAb served as negative controls. The start concentration (1:100 dilution) was 10000 ng/mL for all the mAbs except for F457G2 at 4000 ng/mL. Fig. 1B, Data from End-Point-ELISA of eleven mAbs against SARS-CoV-2 rNP (Wuhan strain) were used for comparison with the ODs from Fig. 1A. The positive control (SARS-CoV-2 immunized mouse serum) was 1:2000 diluted.

(F457G10) to ~0.5 (F461G6) at 1:100 dilution. The four mAbs (F457G9, F457G10, F457G12, and F461G5) that showed negative results in western immunoblot to viruses also had lower reactivity to SARS-CoV-1 rNP, with the ODs between 0.06 and 0.23 at 1:100 dilution, while the other seven mAbs showed ODs from 0.36 to 0.5 (Fig. 1A).

3.5. The binding affinity of mAbs to SARS-CoV-2 nucleocapsid proteins

Endpoint ELISA was used to determine the binding affinity of selected mAbs to rNPs from multiple variants.

All seven tested mAbs showed strong binding to rNPs of the original strain (Wuhan), and the five VOCs. F461G6 and F461G13 had consistently strong binding to rNPs from all the variants, with endpoint titers being 1.25 ng/mL or 2.5 ng/mL. F457G2, F457G3, F459G7, and F461G7 showed slightly variable affinity to rNPs of these variants, with endpoint titers ranging from 1.25 ng/mL to 9.77 ng/mL. While mAb F457G6 had variable affinity to different variants, with endpoint titers from 2.5 ng/mL to 19.5 ng/mL, to rNPs from the original strain (Wuhan strain), or the four earlier circulating VOCs (B.1.1.7, B.1.351, P.1, and B.1.617.2). The affinity to Omicron BA.2 rNP was 78.1 ng/mL, lower than to the other variants. (Table 3).

3.6. Immune plaque assay to confirm the reactivity of mAbs to cultured viruses

The seven mAbs showed variable reactivity to SARS-CoV-2 variants in the immune plaque assay (Table 4, Supplementary Fig. 2). The plaques and intensity of the color observed were graded on a 5-point scale (- to ++++). F457G3, F459G7, F461G6, F461G7, and F461G13, showed strong reactivity to all tested variants, including the reference strain, VOCs B.1.1.7, B.1.351, P.1, B.1.617.2, and Omicron B.1.1.529 and BA.2. F457G2 showed a strong reaction to the reference strain and P.1, but weak reactivity to most variants and non-reaction to B.1.617.2 (Delta variant). In comparison, F457G6 reacted weakly to the reference strain and P.1 and did not respond to the other variants.

3.7. Further verification of the binding affinity of mAbs to recent circulated Omicron sublineages

To verify their reactivity to recently circulating variants, the five mAbs (F457G3, F459G7, F461G6, F461G7, and F461G13) selected from the immune plaque assay were further tested against the rNPs of three Omicron sublineages-BA.4, BQ.1/BQ.1.1, and JN.1 via end-point ELISA (Table 5). Compared to their affinity to the original Wuhan strain, almost all the tested mAbs showed substantially reduced affinity to the two sublineages circulating in 2022 and 2023, with approximately a 16–64 fold increase in end-point concentration for BA.4 (prevalent from June to October 2022) [39], and a 4–8 fold increase for BQ.1/BQ.1.1 (dominant from October 2022 to April 2023) [40,41]. Interestingly, their affinity to the most recent dominant Omicron sublineage JN.1. (prevalent from January to May 2024) [42] was almost the same as to the Wuhan strain.

4. Discussion

The reduced virulence of Omicron coupled with wide-spread vaccination, has substantially decreased COVID-19 associated morbidity and mortality. However, Omicron lineages still threaten vulnerable populations due to their high transmissibility. Early diagnosis of the infection using RAT, followed by antiviral drug treatment, can significantly reduce hospitalization and death [29,32, 37]. Given the rapid mutation of Omicron lineages, however, mAbs with broad recognition capacity are essential for the RAT test.

We generated a panel of nucleocapsid protein-specific mAbs by hybridoma fusion and identified eleven mAbs that showed variable reactivity to selected VOCs by western immunoblot. We then tested their specificity to SARS-CoV-2 NP, compared with rNPs of SARS-CoV-1, MERS, and common human coronaviruses. The affinity of seven mAbs to rNPs of VOCs was verified by EPE. Five mAbs, F461G13, F461G7, F459G7, F457G3, and F461G6 showed strong reactivity to all tested VOCs, including four VOCs (B.1.1.7 (Alpha), B.1.351 (Beta), P.1 (Gamma), B.1.617.2 (Delta)) that circulated during the early phase of the pandemic, and two Omicron sublineages-B.1.1.529 and BA.2. Interestingly, further analysis of these five mAbs' reactivity to Omicron lineages revealed a significant reduction in binding the nucleoproteins of earlier circulating strains BA.4 (prevalent in late 2022) and BQ.1/BQ.1.1 (prevalent in early 2023). However, their affinities to the most recent dominant sublineage JN.1. were similar to the original Wuhan strain (Table 5). The results

Table 3
End-point ELISA to recombinant nucleocapsid proteins (rNPs) from SARS-CoV-2 variants

| MAb | End-point concentration of tested mAbs (ng/mL) | | | | | |
	SARS-Cov-2[a]	B.1.1.7 (Alpha)	B.1.351 (Beta)	P.1 (Gamma)	B.1.617.2 (Delta)	BA.2 (Omicron)
F457G2	4.88	2.5	2.5	2.5	4.88	2.5
F457G3	4.88	4.88	4.88	2.5	4.88	1.25
F457G6	19.5	9.77	4.88	2.5	4.88	78.1
F459G7	9.77	2.5	4.88	4.88	2.5	2.5
F461G6	2.5	1.25	1.25	1.25	1.25	1.25
F461G7	9.77	4.88	9.77	4.88	4.88	2.5
F461G13	2.5	2.5	2.5	1.25	1.25	1.25

[a] original SARS-CoV-2 (Wuhan strain).

Table 4
Plaque assay test of the anti-NP mAbs against SARS-CoV-2 variants

SARS-CoV-2 strains	Antibodies							
	F457G2	F457G3	F457G6	F459G7	F461G6	F461G7	F461G13	Antiserum[d]
Reference strain[a]	++++	++++	++	++++	++++	++++	++++	++
B.1.1.7 (Alpha)	+	++++	–	+++	++++	+++	++	+
B.1.351 (Beta)	+++	++++	–	++++	++++	++++	++++	++
B.1.617.2 (Delta)	–	++++	–	++++	++++	+++	++++	+/++
P.1 (Gamma)	++++	++++	++	++++	++++	++++	++++	++
B.1.1.529[b] **(Omicron)**	+	++++	–	++++	++++	+++/++++	++++	+/++
BA.2[c] **(Omicron)**	+	++++	–	++++	++++	++	++++	++/+++

a, hCoV-19/Canada/ON_ON-VIDO-01-2/2020, EPI_ISL_425177; b, the original Omicron strain; c, Omicron lineage BA.2; d. antiserum from SARS-CoV-2 reference strain immunized mice, used as positive control for hybridoma screening and characterization.

Table 5
End-point ELISA to rNPs from recent circulated Omicron sublineages

mAb	End-point concentration of tested mAbs (ng/mL)		
	BA.4	BQ.1/BQ.1.1	JN.1
F457G3	313	39.1	4.88
F459G7	156	39.1	9.77
F461G6	78.1	19.5	1.25
F461G7	78.1	39.1	9.77
F461G13	39.1	19.5	2.5

indicate that the mutations in NPs from different circulating strains vary over time, highlighting the necessity of closely monitoring RAT sensitivities to each prevalent strain.

Four mAbs (F457G9, F457G10, F457G12, and F461G5) reacted to the rNP of the original strain (Wuhan strain) but showed negative reaction to all tested variants (including the reference strain) in western immunoblot. As these hybridomas were generated from SARS-CoV-2 reference strain immunized mice, the four mAbs were expected to react to the NP of the reference strain. Increasing the loading amount of these four mAbs to 9.6×10^4 PFU did yield a positive response to the reference strain (**Supplement Fig. 1**). Therefore, the negative results in western immunoblot can be explained by the loading amount in SDS-PAGE and the low affinity of these mAbs to virus NPs. These four mAbs were subsequently excluded from EPE and immune plaque analyses.

Except for F461G6 and F461G7, the other nine mAbs also showed negative reactivity to B.1.617.2 (Delta) in western immunoblot (**Table 2**). Given the observation for the four mAbs excluded from EPE and immune plaque assay, it is possible that these nine mAbs might react to the Delta strain if the loading amount was increased. However, we were not able to confirm that because of the low concentration of the Delta variant sample. We did notice a reaction if rNP of the Delta strain to all seven mAbs tested by EPE, indicating that the negative response in western immunoblot was at least partly due to a loading amount issue.

Besides the responses to Delta, the EPE titers of the other variants also showed discordance from the western immunoblot band density. For example, F461G7 showed comparable EPE titers to the rNPs of B.1.1.7 and P.1 (**Table 3**), while having stronger reactivity to P.1 (++++) than to B.1.1.7 (+) in western immunoblot (**Table 2**). One reason for this discrepancy was the antigens used in these studies. The cultured and γ-irradiated virus particles were used in western immunoblot, while rNPs from *E. coli* were used in ELISA. The nucleocapsid proteins from virus and *E. coli* might fold differently, and the phosphorylation and glycosylation modifications also contributed to their discrete antigenic types. In addition, the antigens underwent different treatment in EPE and western immunoblot. In EPE, The rNPs might fold naturally, whereas in western immunoblot, the antigens were denatured due to SDS and heat treatment. Consequently, the mAbs may exhibit different binding affinities to these differently folded antigens. Another possible reason was the blocking buffer used in this study. The buffer in western immunoblot was 5 % skim milk, while the buffer system used in EPE was 0.2 % FBS and 0.2 % skim milk. Different blocking buffer may impact the sensitivity and specificity of the test systems [43,44]. In addition, the concentrations of the secondary antibody were different. A lower concentration (1:5000) was used in western immunoblot, compared to 1:2000 in EPE, which may contribute to the lower reactivity in western immunoblot. A similar discrepancy was also observed between EPE and the immune plaque assay, which may derive from different test conditions, including test antigens, buffer systems, sample concentrations, and substrates.

The specificity of tested mAbs to SARS-CoV-2 NP was confirmed by ELISA to rNPs of SARS-CoV-1, MERS, and four common human coronaviruses HKU1, OC43, NL63 and 229E. Although all mAbs showed negative reactivity to MERS and the four human coronaviruses, several mAbs did show weak reactivity to SARS-CoV-1 rNP. This is not surprising as SARS-CoV-2 NP is 90 % identical to that of SARS-CoV-1 [45,46], and most of the RAT kits authorized by the FDA under EUA can not differentiate the NPs between SARS-CoV and SARS-Cov-2 viruses [37].

The sensitivity and specificity of RAT depends not only on the antibody but also the selected target antigens. SARS-CoV-2 has four major structural proteins: spike protein (S), nucleocapsid protein (N), membrane (M), and envelope protein (E). Spike protein is critical for virus infection and mutates continuously to escape antibody binding. Most of the mAbs generated against the early circulating variants showed reduced titers or complete loss of binding to the later variants, especially after the emergence of Omicron and its

sublineages [47–49]. The E protein is the least abundant in SARS-CoV-2, with only 20 copies per virion [50]. In contrast, nucleocapsid protein is an ideal diagnostic antigen due to the abundance in SARS-CoV-2 virions (about 1000 copies per virion), strong immunogenicity, and comparable conservation among SARS-CoV-2 variants [15,47]. Almost all current FDA-approved RAT kits are based on nucleocapsid protein [37]. The M protein is the most abundant structural protein in SARS-CoV-2 (~2000 copies per virion) [50]. It comprises 222 amino acids, with three transmembrane domains between codons 20–100, and the N-terminal (residues 1–19) and carboxy-terminal (residues 101–222) lying outside and inside the virus envelop respectively [51,52]. This protein is highly conserved across SARS-CoV-2 variants [15], and shares low sequence similarity with common human coronaviruses (Supplemental Table 1) and MERS [53]. Given the potent immunogenicity of M protein in humans, the N- terminal, and especially the long C- terminal, are potential candidates worth exploring for RAT development [54].

In summary, we identified five mAbs (F461G13, F461G7, F459G7, F457G3, and F461G6) showing strong reactivity to all tested VOCs, with minimal reactivity to common human coronaviruses, MERS, and SARS-CoV-1. These mAbs will be further tested against the most recent Omicron sublineages, to verify their capacity to detect emerging variants [17].

Data availability statement

The data associated with this study has not been deposited into a publicly available repository. Data is included in article, supp. Material, and referenced in article.

Ethics approval

This animal studies were approved by the Animal Care Committee of Canadian Science Centre For Human and Animal Health (CSCHAH-ACC) (AUD number H20-017).

Funding

CRediT authorship contribution statement

Hongyu Qiu: Writing – review & editing, Writing – original draft, Supervision, Project administration, Methodology, Investigation, Formal analysis, Conceptualization. **Xin-Yong Yuan:** Writing – review & editing, Validation, Methodology, Investigation, Formal analysis. **Kimberly Holloway:** Writing – review & editing, Validation, Methodology, Investigation, Formal analysis. **Heidi Wood:** Writing – review & editing, Supervision, Methodology, Conceptualization. **Teresa Cabral:** Writing – review & editing, Methodology, Investigation. **Chris Grant:** Writing – review & editing, Methodology, Investigation, Formal analysis. **Peter McQueen:** Writing – review & editing, Methodology, Investigation, Formal analysis. **Garrett Westmacott:** Writing – review & editing, Supervision, Methodology, Conceptualization. **Daniel R. Beniac:** Writing – review & editing, Resources, Methodology. **Lisa Lin:** Writing – review & editing, Resources. **Michael Carpenter:** Writing – review & editing, Resources, Methodology. **Darwyn Kobasa:** Writing – review & editing, Resources. **Tom Gräfenhan:** Writing – review & editing, Supervision, Project administration, Funding acquisition, Conceptualization. **Ian Wayne Cheney:** Writing – review & editing, Supervision, Project administration, Funding acquisition, Conceptualization.

Declaration of competing interest

The authors declare that they have no known competing financial interests or personal relationships that could have appeared to influence the work reported in this paper.

Acknowledgements

Appendix A. Supplementary data

Supplementary data to this article can be found online at https://doi.org/10.1016/j.heliyon.2024.e35325.

References

[1] X. Cui, Y. Wang, J. Zhai, M. Xue, C. Zheng, L. Yu, Future trajectory of SARS-CoV-2: constant spillover back and forth between humans and animals, Virus Res. 328 (2023), https://doi.org/10.1016/j.virusres.2023.199075.

[2] A.M. Carabelli, T.P. Peacock, L.G. Thorne, W.T. Harvey, J. Hughes, T.I. de Silva, S.J. Peacock, W.S. Barclay, T.I. de Silva, G.J. Towers, D.L. Robertson, SARS-CoV-2 variant biology: immune escape, transmission and fitness, Nat. Rev. Microbiol. 21 (2023) 162–177, https://doi.org/10.1038/s41579-022-00841-7.

[3] N. Wolter, W. Jassat, S. Walaza, R. Welch, H. Moultrie, M. Groome, D.G. Amoako, J. Everatt, J.N. Bhiman, C. Scheepers, N. Tebeila, N. Chiwandire, M. du Plessis, N. Govender, A. Ismail, A. Glass, K. Mlisana, W. Stevens, F.K. Treurnicht, Z. Makatini, N. yuan Hsiao, R. Parboosing, J. Wadula, H. Hussey, M.A. Davies, A. Boulle, A. von Gottberg, C. Cohen, Early assessment of the clinical severity of the SARS-CoV-2 omicron variant in South Africa: a data linkage study, Lancet 399 (2022) 437–446, https://doi.org/10.1016/S0140-6736(22)00017-4.

[4] A.C. Ulloa, S.A. Buchan, K.A. Brown, Estimates of SARS-CoV-2 omicron variant severity in ontario, Canada, JAMA 327 (2022) 1286–1288, https://doi.org/10.1001/JAMA.2022.2274.

[5] J.E. Lee, M. Hwang, Y.H. Kim, M.J. Chung, B.H. Sim, W.G. Jeong, Y.J. Jeong, SARS-CoV-2 variants infection in relationship to imaging-based pneumonia and clinical outcomes, Radiology (2023) 306, https://doi.org/10.1148/RADIOL.221795/ASSET/IMAGES/LARGE/RADIOL.221795.TBL4.JPEG.

[6] C. Hyams, R. Challen, R. Marlow, J. Nguyen, E. Begier, J. Southern, J. King, A. Morley, J. Kinney, M. Clout, J. Oliver, S. Gray, G. Ellsbury, N. Maskell, L. Jodar, B. Gessner, J. McLaughlin, L. Danon, A. Finn, A. Langdon, A. Turner, A. Mattocks, B. Osborne, C. Grimes, C. Mitchell, D. Adegbite, E. Bridgeman, E. Scott, F. Perkins, F. Bayley, G. Ruffino, G. Valentine, G. Tilzey, J. Campling, J. Kellett Wright, J. Brzezinska, J. Cloake, K. Milutinovic, K. Helliker, K. Maughan, K. Fox, K. Minou, L. Ward, L. Fleming, L. Morrison, L. Smart, L. Wright, L. Grimwood, M. Bellavia, M. Vasquez, M. Garcia Gonzalez, M. Jeenes-Flanagan, N. Chang, N. Grace, N. Manning, O. Griffiths, P. Croxford, P. Sequenza, R. Lazarus, R. Walters, R. Heath, R. Antico, S. Nammuni Arachchge, S. Suppiah, T. Mona, T. Riaz, V. Mackay, Z. Maseko, Z. Taylor, Z. Friedrich, Z. Szasz-Benczur, Severity of Omicron (B.1.1.529) and Delta (B.1.617.2) SARS-CoV-2 infection among hospitalised adults: a prospective cohort study in Bristol, United Kingdom, The Lancet Regional Health - Europe 25 (2023) 100556, https://doi.org/10.1016/J.LANEPE.2022.100556.

[7] S.K. Greene, A. Levin-Rector, N.T.T. Kyaw, E. Luoma, H. Amin, E. McGibbon, R.W. Mathes, S.D. Ahuja, Comparative hospitalization risk for SARS-CoV-2 Omicron and Delta variant infections, by variant predominance periods and patient-level sequencing results, New York City, August 2021–January 2022, Influenza Other Respir Viruses 17 (2023), https://doi.org/10.1111/irv.13062.

[8] F.P. Esper, T.M. Adhikari, Z.J. Tu, Y.W. Cheng, K. El-Haddad, D.H. Farkas, D. Bosler, D. Rhoads, G.W. Procop, J.S. Ko, L. Jehi, J. Li, B.P. Rubin, Alpha to omicron: disease severity and clinical outcomes of major SARS-CoV-2 variants, JID (J. Infect. Dis.) 227 (2023) 344–352, https://doi.org/10.1093/infdis/jiac411.

[9] N.N.Y. Tsang, H.C. So, B.J. Cowling, G.M. Leung, D.K.M. Ip, Effectiveness of BNT162b2 and CoronaVac COVID-19 vaccination against asymptomatic and symptomatic infection of SARS-CoV-2 omicron BA.2 in Hong Kong: a prospective cohort study, Lancet Infect. Dis. 23 (2023) 421–434, https://doi.org/10.1016/S1473-3099(22)00732-0.

[10] R. Solante, C. Alvarez-Moreno, E. Burhan, S. Chariyalertsak, N.C. Chiu, S. Chuenkitmongkol, D.V. Dung, K.P. Hwang, J. Ortiz Ibarra, S. Kiertiburanakul, P. S. Kulkarni, C. Lee, P.I. Lee, R.C. Lobo, A. Macias, C.H. Nghia, A.L. Ong-Lim, A.J. Rodriguez-Morales, R. Richtmann, M.A.P. Safadi, H.I. Satari, G. Thwaites, Expert review of global real-world data on COVID-19 vaccine booster effectiveness and safety during the omicron-dominant phase of the pandemic, Expert Rev. Vaccines 22 (2023) 1–16, https://doi.org/10.1080/14760584.2023.2143347.

[11] I.L. Ward, C. Bermingham, D. Ayoubkhani, O.J. Gethings, K.B. Pouwels, T. Yates, K. Khunti, J.L. Hippisley-Cox, A. Banerjee, A.S. Walker, V. Nafilyan, Risk of covid-19 related deaths for SARS-CoV-2 omicron (B.1.1.529) compared with delta (B.1.617.2): retrospective cohort study, BMJ 378 (2022), https://doi.org/10.1136/BMJ-2022-070695.

[12] Z.H. Strasser, N. Greifer, A. Hadavand, S.N. Murphy, H. Estiri, Estimates of SARS-CoV-2 omicron BA.2 subvariant severity in new England, JAMA Netw. Open 5 (2022), https://doi.org/10.1001/JAMANETWORKOPEN.2022.38354.

[13] S. Adjei, K. Hong, N.-A.M. Molinari, Lara Bull-Otterson, U.A. Ajani, A. V Gundlapalli, A.M. Harris, Joy Hsu, Sameer, S. Kadri, J. Starnes, K. Yeoman, T. K. Boehmer, Morbidity and Mortality Weekly Report Mortality Risk Among Patients Hospitalized Primarily for COVID-19 during the Omicron and Delta Variant Pandemic Periods-United States, 2022.

[14] Y. Liu, J. Rocklöv, The effective reproductive number of the Omicron variant of SARS-CoV-2 is several times relative to Delta, J Travel Med 29 (2022) 1–4, https://doi.org/10.1093/JTM/TAAC037.

[15] Y. Fan, X. Li, L. Zhang, S. Wan, L. Zhang, F. Zhou, SARS-CoV-2 Omicron variant: recent progress and future perspectives, Signal Transduct Target Ther 7 (2022), https://doi.org/10.1038/s41392-022-00997-x.

[16] World Health Organization, WHO Coronavirus (COVID-19) Dashboard | WHO Coronavirus (COVID-19) Dashboard With Vaccination Data, (n.d.). https://covid19.who.int/(accessed March 8, 2023).

[17] Centers for Disease Control and Prevention, COVID Data Tracker, 2023. https://covid.cdc.gov/covid-data-tracker/#trends_totaldeaths_select_00. (Accessed 10 March 2023).

[18] J. Paget, P. Spreeuwenberg, V. Charu, R.J. Taylor, A.D. Iuliano, J. Bresee, L. Simonsen, C. Viboud, Global mortality associated with seasonal influenza epidemics: new burden estimates and predictors from the GLaMOR Project, J Glob Health 9 (2019), https://doi.org/10.7189/JOGH.09.020421.

[19] World Health Organization, Up to 650 000 people die of respiratory diseases linked to seasonal flu each year, (n.d.). https://www.who.int/news/item/13-12-2017-up-to-650-000-people-die-of-respiratory-diseases-linked-to-seasonal-flu-each-year (accessed March 8, 2023).

[20] R.M. Fericean, C. Oancea, A.R. Reddyreddy, O. Rosca, F. Bratosin, V. Bloanca, C. Citu, S. Alambaram, N.G. Vasamsetti, C. Dumitru, Outcomes of elderly patients hospitalized with the SARS-CoV-2 omicron B.1.1.529 variant: a systematic review, Int J Environ Res Public Health 20 (2023), https://doi.org/10.3390/ijerph20032150.

[21] B. Long, B.M. Carius, S. Chavez, S.Y. Liang, W.J. Brady, A. Koyfman, M. Gottlieb, Clinical update on COVID-19 for the emergency clinician: presentation and evaluation, Am. J. Emerg. Med. 54 (2022) 46–57, https://doi.org/10.1016/J.AJEM.2022.01.028.

[22] Centers for Disease Control and Prevention, COVID-19 prevention actions. https://www.cdc.gov/coronavirus/2019-ncov/prevent-getting-sick/prevention.html#ventilation, 2023. (Accessed 17 December 2023).

[23] X. Li, M. Xiong, Q. Deng, X. Guo, Y. Li, The utility of SARS-CoV-2 nucleocapsid protein in laboratory diagnosis, J. Clin. Lab. Anal. 36 (2022) e24534, https://doi.org/10.1002/JCLA.24534.

[24] T. Peto, D. Affron, B. Afrough, A. Agasu, M. Ainsworth, A. Allanson, K. Allen, C. Allen, L. Archer, N. Ashbridge, I. Aurfan, M. Avery, E. Badenoch, P. Bagga, R. Balaji, E. Baldwin, S. Barraclough, C. Beane, J. Bell, T. Benford, S. Bird, M. Bishop, A. Bloss, R. Body, R. Boulton, A. Bown, C. Bratten, C. Bridgeman, D. Britton, T. Brooks, M. Broughton-Smith, P. Brown, B. Buck, E. Butcher, W. Byrne, G. Calderon, S. Campbell, O. Carr, P. Carter, D. Carter, M. Cathrall, M. Catton, J. Chadwick, D. Chapman, K.K. Chau, T. Chaudary, S. Chidavaenzi, S. Chilcott, B. Choi, H. Claasen, S. Clark, R. Clarke, D. Clarke, R. Clayton, K. Collins, R. Colston, J. Connelly, E. Cook, M. Corcoran, B. Corley, L. Coulson, C. Coulson, A. Crook, D.W. Crook, S. D'Arcangelo, M.A. Darby, R. de Koning, P. Derbyshire, P. Devall, M. Dolman, N. Draper, M. Driver, S. Dyas, E. Eaton, J. Edwards, R. Elderfield, K. Ellis, G. Ellis, S. Elwell, R. Evans, B. Evans, M. Evans, R. Evans, D. Eyre, C. Fahey, V. Fenech, J. Field, A. Field, T. Foord, T. Fowler, M. French, H. Fuchs, J. Gan, J. Gernon, G. Ghadiali, N. Ghuman, K. Gibbons, G. Gill, K. Gilmour, A. Goel, S. Gordon, T. Graham, A. Grassam-Rowe, D. Green, A. Gronert, T. Gumsley-Read, C. Hall, B. Hallis, S. Hammond, P. Hammond, B. Hanney, V. Hardy, G. Harker, A. Harris, M. Havinden-Williams, E. Hazell, J. Henry, K. Hicklin, K. Hollier, B. Holloway, S.J. Hoosdally, S. Hopkins, L. Hughes, S. Hurdowar, S.A. Hurford, J. Jackman, H. Jackson, R. Johns, S. Johnston, J. Jones, T. Kanyowa, K. Keating-Fedders, S. Kempson, I. Khan, B. Khulusi, T. Knight, A. Krishna, P. Lahert, Z. Lampshire, D. Lasserson, K. Lee, L.Y.W. Lee, A. Legard, C. Leggio, J. Liu, T. Lockett, C. Logue, V. Lucas, S. F. Lumley, V. Maripuri, D. Markham, E. Marshall, P.C. Matthews, S. Mckee, D.F. McKee, N. McLeod, A. McNulty, F. Mellor, R. Michel, A. Mighiu, J. Miller, Z. Mirza, H. Mistry, J. Mitchell, M.E. Moeser, S. Moore, A. Muthuswamy, D. Myers, G. Nanson, M. Newbury, S. Nicol, H. Nuttall, J.J. Nwanaforo, L. Oliver, W. Osbourne, J. Osbourne, A. Otter, J. Owen, S. Panchalingam, D. Papoulidis, J.D. Pavon, A. Peace, K. Pearson, L. Peck, A. Pegg, S. Pegler, H. Permain, P. Perumal, L. Peto, T.E.A. Peto, T. Pham, H.L. Pickford, M. Pinkerton, M. Platton, A. Price, E. Protheroe, H. Purnell, L. Rawden, S. Read, C. Reynard, S. Ridge, T.

G. Ritter, J. Robinson, P. Robinson, G. Rodger, C. Rowe, B. Rowell, A. Rowlands, S. Sampson, K. Saunders, R. Sayers, J. Sears, R. Sedgewick, L. Seeney, A. Selassie, L. Shail, J. Shallcross, L. Sheppard, A. Sherkat, S. Siddiqui, A. Sienkiewicz, L. Sinha, J. Smith, E. Smith, E. Stanton, T. Starkey, A. Stawiarski, A. Sterry, J. Stevens, M. Stockbridge, N. Stoesser, A. Sukumaran, A. Sweed, S. Tatar, H. Thomas, C. Tibbins, S. Tiley, J. Timmins, C. Tomas-Smith, O. Topping, E. Turek, T. Neibler, K. Trigg-Hogarth, E. Truelove, C. Turnbull, D. Tyrrell, A. Vaughan, J. Vertannes, R. Vipond, L. Wagstaff, J. Waldron, P. Walker, A.S. Walker, M. Walters, J.Y. Wang, E. Watson, K. Webberley, K. Webster, G. Westland, I. Wickens, J. Willcocks, H. Willis, S. Wilson, B. Wilson, L. Woodhead, D. Wright, B. Xavier, F. Yelnoorkar, L. Zeidan, R. Zinyama, COVID-19: rapid antigen detection for SARS-CoV-2 by lateral flow assay: a national systematic evaluation of sensitivity and specificity for mass-testing, EClinicalMedicine 36 (2021) 100924, https://doi.org/10.1016/j.eclinm.2021.100924.

[25] F.J. Chadwick, J. Clark, S. Chowdhury, T. Chowdhury, D.J. Pascall, Y. Haddou, J. Andrecka, M. Kundegorski, C. Wilkie, E. Brum, T. Shirin, A.S.M. Alamgir, M. Rahman, A.N. Alam, F. Khan, B. Swallow, F.S. Mair, J. Illian, C.L. Trotter, D.L. Hill, D. Husmeier, J. Matthiopoulos, K. Hampson, A. Sania, Combining rapid antigen testing and syndromic surveillance improves community-based COVID-19 detection in a low-income country, Nat. Commun. 13 (2022), https://doi.org/10.1038/s41467-022-30640-w.

[26] The U.S. Food and Drug Administration (FDA), SARS-CoV-2 Viral Mutations: Impact on COVID-19 Tests | FDA, (n.d.). https://www.fda.gov/medical-devices/coronavirus-covid-19-and-medical-devices/sars-cov-2-viral-mutations-impact-covid-19-tests (accessed March 9, 2023).

[27] R.P. Venekamp, E. Schuit, L. Hooft, I.K. Veldhuijzen, W. van den Bijllaardt, S.D. Pas, V.F. Zwart, E.B. Lodder, M. Hellwich, M. Koppelman, R. Molenkamp, C.J. H. Wijers, I.H. Vroom, L.C. Smeets, C.R.S. Nagel-Imming, W.G.H. Han, S. van den Hof, J.A.J.W. Kluytmans, J.H.H.M. van de Wijgert, K.G.M. Moons, Diagnostic accuracy of SARS-CoV-2 rapid antigen self-tests in asymptomatic individuals in the omicron period: a cross-sectional study, Clin. Microbiol. Infection 29 (2023) 391.e1–391.e7, https://doi.org/10.1016/j.cmi.2022.11.004.

[28] E. Schuit, R.P. Venekamp, L. Hooft, I.K. Veldhuijzen, W. Van Den Bijllaardt, S.D. Pas, V.F. Zwart, E.B. Lodder, M. Hellwich, M. Koppelman, R. Molenkamp, C.J. H. Wijers, I.H. Vroom, L.C. Smeets, C.R.S. Nagel-Imming, W.G.H. Han, S. Van Den Hof, J.A.J.W. Kluytmans, J.H.H.M. Van De Wijgert, K.G.M. Moons, Diagnostic accuracy of covid-19 rapid antigen tests with unsupervised self-sampling in people with symptoms in the omicron period: cross sectional study, BMJ 378 (2022), https://doi.org/10.1136/BMJ-2022-071215.

[29] X. Zhang, B. Barr, M. Green, D. Hughes, M. Ashton, D. Charalampopoulos, M. García-Fiñana, I. Buchan, Impact of community asymptomatic rapid antigen testing on covid-19 related hospital admissions: synthetic control study, BMJ 379 (2022), https://doi.org/10.1136/BMJ-2022-071374.

[30] J. Hammond, H. Leister-Tebbe, A. Gardner, P. Abreu, W. Bao, W. Wisemandle, M. Baniecki, V.M. Hendrick, B. Damle, A. Simón-Campos, R. Pypstra, J. M. Rusnak, Oral nirmatrelvir for high-risk, nonhospitalized adults with covid-19, N. Engl. J. Med. 386 (2022) 1397–1408, https://doi.org/10.1056/NEJMOA2118542/SUPPL_FILE/NEJMOA2118542_DATA-SHARING.PDF.

[31] A. Jayk Bernal, M.M. Gomes da Silva, D.B. Musungaie, E. Kovalchuk, A. Gonzalez, V. Delos Reyes, A. Martín-Quirós, Y. Caraco, A. Williams-Diaz, M.L. Brown, J. Du, A. Pedley, C. Assaid, J. Strizki, J.A. Grobler, H.H. Shamsuddin, R. Tipping, H. Wan, A. Paschke, J.R. Butterton, M.G. Johnson, C. De Anda, Molnupiravir for oral treatment of covid-19 in nonhospitalized patients, N. Engl. J. Med. 386 (2022) 509–520, https://doi.org/10.1056/nejmoa2116044.

[32] C.K.H. Wong, I.C.H. Au, K.T.K. Lau, E.H.Y. Lau, B.J. Cowling, G.M. Leung, Real-world effectiveness of early molnupiravir or nirmatrelvir–ritonavir in hospitalised patients with COVID-19 without supplemental oxygen requirement on admission during Hong Kong's omicron BA.2 wave: a retrospective cohort study, Lancet Infect. Dis. 22 (2022) 1681–1693, https://doi.org/10.1016/S1473-3099(22)00507-2.

[33] L. Vangeel, W. Chiu, S. De Jonghe, P. Maes, B. Slechten, J. Raymenants, E. André, P. Leyssen, J. Neyts, D. Jochmans, Remdesivir, Molnupiravir and Nirmatrelvir remain active against SARS-CoV-2 Omicron and other variants of concern, Antivir. Res. 198 (2022) 105252, https://doi.org/10.1016/J.ANTIVIRAL.2022.105252.

[34] Z.E. Mohammadie, S. Akhlaghi, S. Samaeinasab, S. Shaterzadeh-Bojd, T. Jamialahmadi, A. Sahebkar, Clinical performance of rapid antigen tests in comparison to RT-PCR for SARS-COV-2 diagnosis in Omicron variant: a systematic review and meta-analysis, Rev. Med. Virol. 33 (2023) e2428, https://doi.org/10.1002/RMV.2428.

[35] K. Leuzinger, T. Roloff, A. Egli, H.H. Hirsch, Impact of SARS-CoV-2 omicron on rapid antigen testing developed for early-pandemic SARS-CoV-2 variants, Microbiol. Spectr. 10 (2022), https://doi.org/10.1128/spectrum.02006-22.

[36] P. Jüni, S. Baert, A. Corbeil, J. Johnstone, S.N. Patel, P. Bobos, U. Allen, K.A. Barrett, L.L. Barrett, N.S. Bodmer, K.B. Born, L. Bourns, G.A. Evans, J. Hopkins, D. G. Manuel, A.M. Morris, F. Razak, B. Sander, M. Science, R. Steiner, J. Tepper, N. Thampi, A. McGeer, Use of rapid antigen tests during the omicron wave. https://doi.org/10.47326/OCSAT.2022.03.56.1.0, 2022.

[37] The U.S. Food and Drug Administration (FDA), In vitro Diagnostics EUAs - Antigen Diagnostic Tests for SARS-CoV-2 | FDA, (n.d.). https://www.fda.gov/medical-devices/covid-19-emergency-use-authorizations-medical-devices/in-vitro-diagnostics-euas-antigen-diagnostic-tests-sars-cov-2 (accessed March 8, 2023).

[38] H. Qiu, X.Y. Yuan, T. Cabral, K. Manguiat, A. Robinson, H. Wood, C. Grant, P. McQueen, G. Westmacott, D.R. Beniac, L. Lin, M. Carpenter, D. Kobasa, T. Gräfenhan, Development and characterization of SARS-CoV-2 variant-neutralizing monoclonal antibodies, Antivir. Res. 196 (2021) 105206, https://doi.org/10.1016/J.ANTIVIRAL.2021.105206.

[39] Outbreak.info. BA.4 lineage report. https://outbreak.info/situation-reports?pango=BA.4&loc=USA&loc=USA_US-CA&selected=Worldwide&overlay=false. (Accessed 17 June 2024).

[40] Outbreak.info. BQ.1 lineage report. https://outbreak.info/situation-reports?pango=BQ.1&loc=USA&loc=USA_US-CA&selected=Worldwide&overlay=false. (Accessed 20 June 2024).

[41] Outbreak.info. BQ.1.1 lineage report. https://outbreak.info/situation-reports?pango=BQ.1.1&loc=USA&loc=USA_US-CA&selected=Worldwide&overlay=false. (Accessed 20 June 2024).

[42] Centers for Disease Control and Prevention, COVID data tracker, variant proportions. https://covid.cdc.gov/covid-data-tracker/#variant-proportions. (Accessed 20 June 2024).

[43] T. Mahmood, P.C. Yang, Western blot: technique, theory, and trouble shooting, N. Am. J. Med. Sci. 4 (2012) 429, https://doi.org/10.4103/1947-2714.100998.

[44] Y. Xiao, S.N. Isaacs, Enzyme-linked immunosorbent assay (ELISA) and blocking with bovine serum albumin (BSA)—not all BSAs are alike, J. Immunol. Methods 384 (2012) 148–151, https://doi.org/10.1016/J.JIM.2012.06.009.

[45] A. Grifoni, J. Sidney, Y. Zhang, R.H. Scheuermann, B. Peters, A. Sette, A sequence homology and bioinformatic approach can predict candidate targets for immune responses to SARS-CoV-2, Cell Host Microbe 27 (2020) 671–680.e2, https://doi.org/10.1016/j.chom.2020.03.002.

[46] B. Tilocca, A. Soggiu, M. Sanguinetti, V. Musella, D. Britti, L. Bonizzi, A. Urbani, P. Roncada, Comparative computational analysis of SARS-CoV-2 nucleocapsid protein epitopes in taxonomically related coronaviruses, Microbes Infect 22 (2020) 188–194, https://doi.org/10.1016/J.MICINF.2020.04.002.

[47] M. Shah, H.G. Woo, Omicron: a heavily mutated SARS-CoV-2 variant exhibits stronger binding to ACE2 and potently escapes approved COVID-19 therapeutic antibodies, Front. Immunol. 12 (2022) 830527, https://doi.org/10.3389/FIMMU.2021.830527/BIBTEX.

[48] M.G. Cox, T.P. Peacock, W.T. Harvey, J. Hughes, D.W. Wright, B.J. Willett, E. Thomson, R.K. Gupta, S.J. Peacock, D.L. Robertson, A.M. Carabelli, SARS-CoV-2 variant evasion of monoclonal antibodies based on in vitro studies, Nat. Rev. Microbiol. 21 (2023) 112–124, https://doi.org/10.1038/s41579-022-00809-7.

[49] M.S. Alam, Insight into SARS-CoV-2 Omicron variant immune escape possibility and variant independent potential therapeutic opportunities, Heliyon 9 (2023) e1385, https://doi.org/10.1016/j.heliyon.2023.e13285.

[50] Y.M. Bar-On, A. Flamholz, R. Phillips, R. Milo, Sars-cov-2 (Covid-19) by the numbers, Elife 9 (2020), https://doi.org/10.7554/eLife.57309.

[51] I.M. Artika, A.K. Dewantari, A. Wiyatno, Molecular biology of coronaviruses: current knowledge, Heliyon 6 (2020) e04743, https://doi.org/10.1016/j.heliyon.2020.e04743.

[52] R. Gorkhali, P. Koirala, S. Rijal, A. Mainali, A. Baral, H.K. Bhattarai, Structure and function of major SARS-CoV-2 and SARS-CoV proteins, Bioinf. Biol. Insights 15 (2021), https://doi.org/10.1177/11779322211025876.

[53] S. Thomas, The structure of the membrane protein of SARS-CoV-2 resembles the sugar transporter SemiSWEET, Pathog Immun 5 (2020) 342–363, https://doi.org/10.20411/PAI.V5I1.377.

[54] Z. Lopandić, I. Protić-Rosić, A. Todorović, S. Glamočlija, M. Gnjatović, D. Ćujic, M. Gavrović-Jankulović, Igm and igg immunoreactivity of sars-cov-2 recombinant m protein, Int. J. Mol. Sci. 22 (2021), https://doi.org/10.3390/ijms22094951.